Guest-induced Reversible Transformation between an Azulene-based Pd_2L_4 Lantern-shaped Cage and a Pd_4L_8 Tetrahedron

Alexandre Walther,[1] Irene Regeni,[1,2] Julian J. Holstein[1] and Guido H. Clever[1*]

[1] Department of Chemistry and Chemical Biology, TU Dortmund University, Otto Hahn Str. 6, 44227 Dortmund, Germany.

[2] Leiden Institute of Chemistry, Leiden University, Einsteinweg 55, 2333CC Leiden, The Netherlands

ABSTRACT: Azulene, a blue-colored structural isomer of naphthalene, is introduced as the backbone for a new family of Pd(II)-based self-assemblies. Three organic ligands, equipped with varying donor groups, produce three [Pd_2L_4] cages of different cavity dimensions. Unexpectedly, addition of organic disulfonate guests to the smallest lantern-shaped cage (featuring pyridine donors) led to a rapid and quantitative transformation to a distorted-tetrahedral [Pd_4L_8] species. On the contrary, [Pd_2L_4] cages formed from ligands with isoquinoline donors either just encapsulated the guests or showed no interaction. The tetrahedral species could be fully reverted back to its original [Pd_2L_4] topology by capturing the guest by another, stronger binding [$Pd_2L'_4$] coordination cage, narcissistically self-sorting from the first cage. The azulenes, serving as colored hydrocarbon backbones of minimal atom count, allow to follow cage assembly and guest-induced transformation by the naked eye. Furthermore, we propose that their peculiar electronic structure influences the system's assembly behavior.

INTRODUCTION

Coordination cages and related metal-organic assemblies have turned into a significative subfield of supramolecular chemistry over the last decades.[1] Many different shapes and topologies have been prepared, ranging from simple "lantern-shaped" cages[2–5] to large spheres,[6] as well as squares,[7,8] tetrahedra,[9–11] knots,[12–15] catenanes[16–18] and further topologies.

Cages with an accessible cavity can act as nanoscopic hosts for guest molecules,[19–22] making them comparable to biological receptors and enzymes.[23] Artificial enzyme mimics formed by coordination cages have been reported.[23] One notable difference between most coordination cages and peptidic receptors is the structural flexibility of the latter ones: enzymes often respond to substrates by adapting their binding sites to an optimal conformation and size, even leading to extensive refolding and multimerization processes.

While most reports on the binding of guest molecules in the cavities of coordination cages have demonstrated that guest uptake does not affect topology and nuclearity of the final complex, a few examples of coordination chemistry-based hosts showing significant size and shape transformation upon guest uptake are found in the literature. A notable early example was described by the Raymond group in 1999 where they showed that a Ti(IV) or Ga(III)-based triple stranded helicate converts to a tetrahedral cage upon binding a tetrabutylammonium cation, thereby doubling the number of components per complex.[24] Subsequently, other examples of guest-triggered transformations were reported for guests such as fullerenes,[25] halides,[26] and various inorganic anions,[27,28] as recently reviewed by Percástegui[29] and Nitschke.[30]

Here we introduce a new system capable of undergoing a fully reversible guest-triggered transformation from a [Pd_2**L**$_4$] lantern-shaped coordination cage to a larger [Pd_4**L**$_8$] distorted tetrahedron. The quantitative, and rapid reversibility of this system contrasts with previous reports on cage transformations where reversibility was, for example, not explored[31] or resulted in an unfavorable equilibrium state.[32]

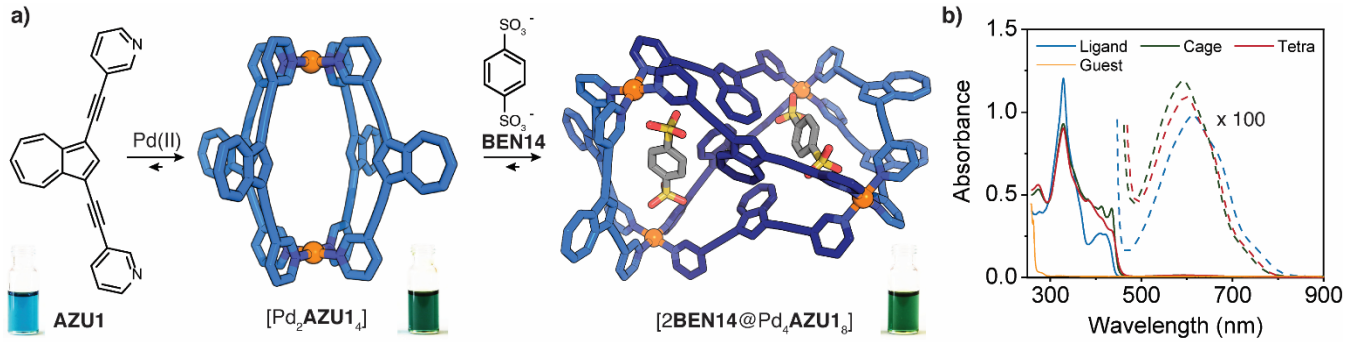

Figure 1. (a) X-ray structures of (left) cage [Pd_2(**AZU1**)$_4$] and (right) tetrahedron [2**BEN14**@Pd_4(**AZU1**)$_8$], (counter-anions, solvents and disorders omitted for clarity) and photographs of the corresponding species in DMSO solution. (b) Absorption spectra of the three species and of **BEN14**. Dashed lines represent the visible region absorption bands above 420-450 nm (π-π* transitions), zoomed in 100x.

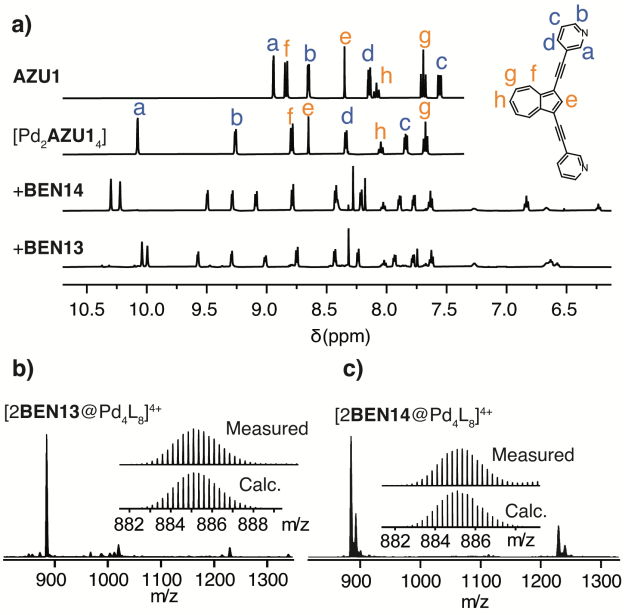

Figure 2. (a) ^{1}H-NMR spectra (600MHz, 298K, DMSO-d_6) of, from top to bottom, ligand **AZU1**, cage [Pd_2(**AZU1**)$_4$], tetrahedron [2**BEN14**@Pd_4(**AZU1**)$_8$] and tetrahedron [2**BEN13**@Pd_4(**AZU1**)$_8$]. (b) HR-ESI-MS of tetrahedron [2**BEN13**@Pd_4(**AZU1**)$_8$]$^{4+}$ (left) and tetrahedron [2**BEN14**@Pd_4(**AZU1**)$_8$]$^{4+}$ (right). The counter anion is OTf$^-$ in all coordination species.

In addition, the trigger for the reverse transformation in our case is a second, different [Pd_2**L**$_4$] cage capable of narcissistically self-sorting and able to "steal" the guest from the first cage. To the best of our knowledge, such an approach has never been used before to drive assembly transformation. It further enriches the growing number of tools aimed at bestowing dynamic Pd-based assemblies and host-guest complexes with stimuli-responsive, emergent and 'systems chemistry' behavior.

RESULTS AND DISCUSSIONS

The initial [Pd_2**L**$_4$] cage is constructed from ligands based on azulene, a blue-colored structural isomer of naphthalene. Due to its peculiar electronic structure, comprising a seven-membered fused to a five-membered ring, azulene features a strong dipole moment of 1.08 Debye,[33] highly unusual for purely hydrocarbon aromatics.[34] We herein show that this feature has both implications on the course as well as visible monitoring of the assembly process.

Ligand **AZU1** was synthesized *via* Sonogashira coupling between 1,3-dibromoazulene[35] and 3-ethynylpyridine. Ligands **AZU2** and **AZU3** were synthesized similarly using 8- and 7-ethynylisoquinoline. Owing to their azulene cores, all three ligands are intensely colored, between teal and green (see photographs in Figs. 1 and 3). The full synthetic pathways are described in the Supplementary Information.

Quantitative formation of the [Pd_2**L**$_4$] cages was achieved by combining the ligands and the palladium(II) salts [$Pd(CH_3CN)_4$]OTf_2 or [$Pd(CH_3CN)_4$]$(BF_4)_2$ in a 2:1 ratio in DMSO-d_6 or CD_3CN and heating at 70 °C for 15 min. In accordance with our previously reported lantern-shaped Pd(II) cages,[10,36–38] assembly formation was indicated by a significant downfield shift of the donor groups' proton signals, especially for the two protons neighboring the coordination sites Ha and Hb (Fig. 2a). Moreover, formation of the cages was visually indicated by a color change of the solutions, going from teal to green for **AZU1** and **AZU3** and from green to brown for **AZU2** (see photographs in Figs. 1 and 3). In addition, ESI-MS analysis gave evidence of the formation of cages with [Pd_2L_4] stoichiometry (Figs. S11, S16 and S22). Finally, single crystals suitable for X-ray diffraction were obtained for species [Pd_2**AZU1**$_4$] by slow diffusion of ethyl acetate in its DMSO solution (Fig. 1), and for [Pd_2**AZU2**$_4$] by slow diffusion of diisopropylether in its acetonitrile solution (Fig. 3a). [Pd_2**AZU1**$_4$] adopts a lantern shape similar to previously reported structures,[5] while [Pd_2**AZU2**$_4$], due to its 8-isoquinoline donor groups, adopts a helical shape.[39] Interestingly, in the latter structure both helical isomers co-crystallize as closely packed pairs, where the aromatic regions of both enantiomers stack together and therefore yield a distorted geometry (Fig. S55).

Next, the interaction of the positively charged coordination cages with negatively charged guests was studied. Benzene-1,4- (**BEN14**) and 1,3- (**BEN13**) disulfonate were used as tetrabutylammonium salts in DMSO-d_6 for solubility reasons. Firstly, helicate [Pd_2**AZU2**$_4$] showed no encapsulation of either guest, owing probably to its small cavity. [Pd_2**AZU3**$_4$] exhibited encapsulation of both guests, as observed by NMR and ESI-MS experiments (Fig. 3d and S41-S45). However, rapid precipitation after the addition of one equivalent of guest precluded the determination of binding constants by ^{1}H-NMR titration. The data, however, unambiguously indicates the system to be in the fast exchange regime. By UV/Vis titration, the binding constant could be determined to be K_{11} = 6557 ± 273 M^{-1} (Fig. S46). The [**BEN14**@Pd_2**AZU3**$_4$] host-guest complex could be crystallized by slow vapor diffusion of toluene into the DMSO solution and analyzed by single-crystal X-ray diffraction (Fig. 3c): guest **BEN14** sits in the middle of the cavity of the cage, with its sulfonate groups pointing towards the nearest palladium atom due to electrostatic interactions.[4]

Finally, the addition of 1 equivalent of either **BEN14** or **BEN13** to a DMSO solution of [Pd_2**AZU1**$_4$] yielded new species after 5 minutes of heating at 70 °C. These showed a 1:1 splitting of all ^{1}H-NMR signals (Fig. 2a), indicating the formation of a new species, which was confirmed by ESI-MS analysis. It is worth noting that complete guest-triggered transformation was only observed when using OTf$^-$ as a counter anion; if BF_4^- was used, the addition of 1 eq. of guest only led to a conversion of approx. 66% (by NMR integration) and, additionally, precipitation was also observed (Fig. S28). This behavior is probably caused by competitive encapsulation of BF_4^-, preventing the disulfonate guest to fully bind inside the cage, while larger OTf$^-$ is not as competitive. In addition, DMSO-d_6 was the only solvent where this transformation was possible; fast precipitation was observed upon addition of the guests in CD_3CN or DMF-d_7.

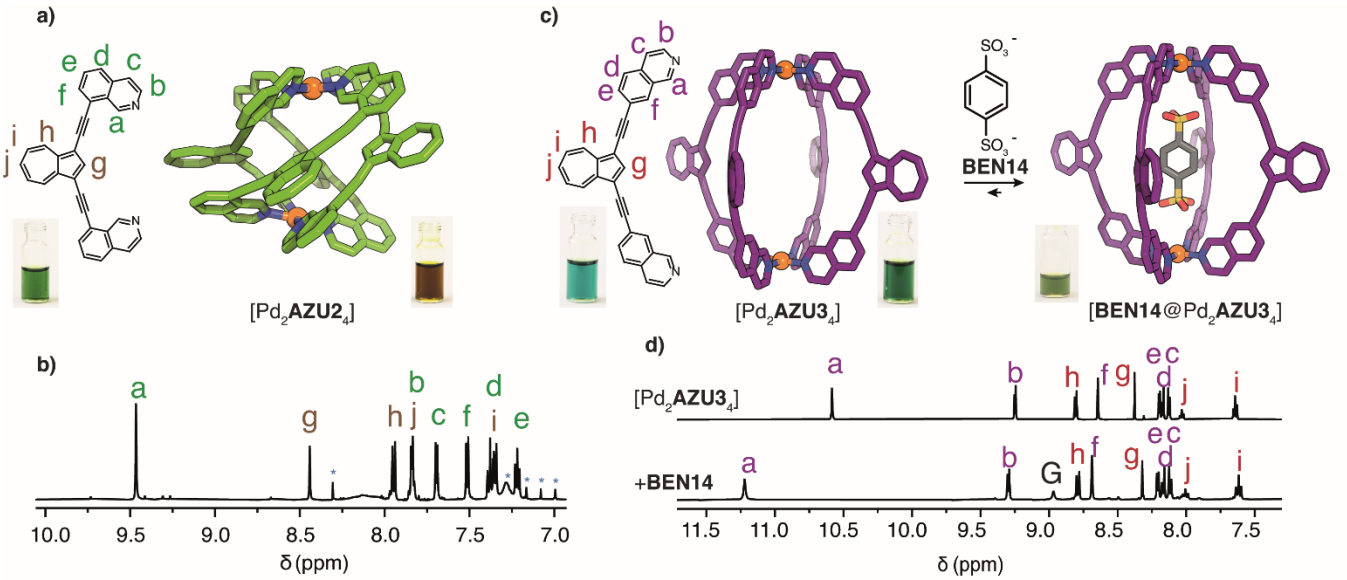

Figure 3. (a) X-ray structure of helicate [Pd_2(**AZU2**)$_4$] and (b) its ^{1}H-NMR spectrum (600MHz, 298K, CD_3CN; blue stars indicate impurities). (c) Encapsulation of guest **BEN14** in cage [Pd_2(**AZU3**)$_4$] and X-ray structure of the host-guest complex. (d) ^{1}H-NMR spectra (600MHz, 298K, DMSO-d_6) of cage [Pd_2(**AZU3**)$_4$] (top) and host-guest complex [**BEN14**@Pd_2(**AZU3**)$_4$] after the addition of 1 eq. of guest (bottom; G = guest). Photographs of ligand and cage solutions are shown.

The ESI-MS analysis confirmed that a doubling of the atomic count as well as an encapsulation of two guest molecules had taken place in the newly formed species, which therefore has a formula of [2**G**@Pd_4**AZU1**$_8$]$^{4+}$, where **G** indicates either guest **BEN13** or **BEN14** (Fig. 2b).

Moreover, Diffusion Ordered SpectroscopY (DOSY) NMR revealed an increase of the hydrodynamic radii from 10.5 Å to 13.2 Å and 14.3 Å for the newly formed species, respectively, containing **BEN13** or **BEN14** (Fig. S32).

The color of the solution also changed during the transformation, going from a dark green to a lighter shade. The difference is difficult to capture by photography (Fig. 1), however, UV-Vis spectroscopy unambiguously confirmed a spectral change upon guest binding. We suppose that the observed color changes between the species correlate with the sensitivity of azulene towards its electronic environment.[40,41]

Knowing the composition and approximate size of the newly formed [2**G**@Pd_4**AZU1**$_8$]$^{4+}$ species, we then wondered about its actual structure. A number of different topologies of M_4L_8 species have been described to date: quadruply interlocked [Pd_2**L**$_4$] double-cages,[42] squares with two ligands per edge,[43] pseudo-tetrahedra,[44] and a twisted assembly of two doubly bridged [Pd_2**L**$_3$] bowls.[45] Of those four topologies, only the mechanically interlocked cages and the tetrahedra are expected to show a 1:1 splitting pattern of the ligands' NMR signals upon coordination (compare, however, Lützen's chiral [Pd_4**L**$_8$] squares[46]). Due to the rather short ligands and large guests we could rule out the interlocked topology and inferred the formation of a tetrahedral species, able to explain the observed 1:1 NMR signal splitting.[10] We first determined this topology though a 2D ^{1}H-NMR analysis (Fig. S26) and later confirmed this topology thanks to X-ray structural analysis of single crystals grown from a 1:1 mixture of a 0.35 mM solution of the tetrahedron with **BEN14** as the guest in DMSO-*d*$_6$, and a 15 mM solution of NBu_4ReO_4 by slow vapor diffusion of toluene into the mother liquor (Fig. 1). The asymmetric unit contains two tetrahedra, two ReO_4^- anions, seven **BEN14** guests, as well as DMSO and toluene solvent molecules. Expanding the solid-state packing reveals that the two different tetrahedra are grouped as pairs (A and B) joined by stacking of some of their azulene subunits. Moreover, one can observe that in one of the tetrahedra, the **BEN14** guests are aligned parallel to the closest Pd-Pd axis, while in the second tetrahedron, one of the guests is pointing outside of the structure with one of its sulfonate groups.

Analysis of the cavity volumes of the different structures reveals that the guests benefit from larger cavities in the tetrahedron as compared to the [Pd_2**AZU1**$_4$] cage (321-345 Å^3 vs. 221 Å^3 per cavity; Table S3 and Fig. S58). The distance between the Pd atoms also increases from 12.3 Å in the cage to 14.0 Å (shortest) in the tetrahedron. This increase in volume and space between the two cations may be one of the driving forces for the observed transformation from cage to tetrahedron, thereby maximizing the attractive interactions between all the components.[47]

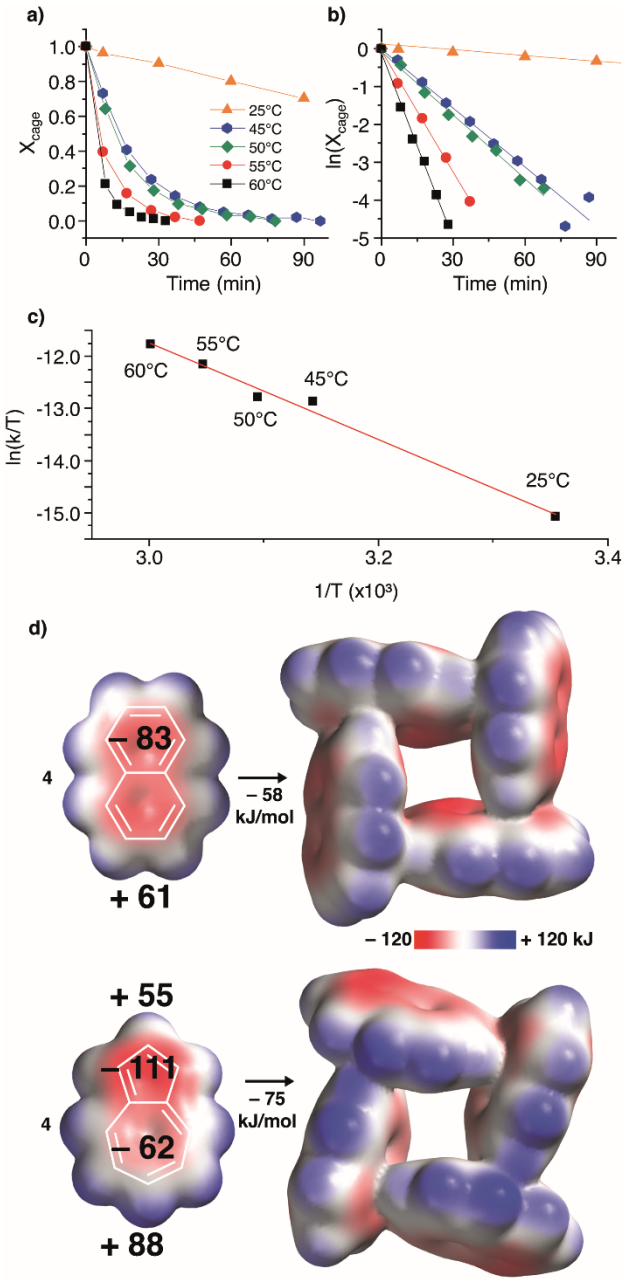

Figure 4. Cage conversion in solution: (a) [Pd_2(**AZU1**)$_4$] fraction and (b) ln[cage fraction] over time measured by NMR with linear regression. (c) Eyring plot with rate constants determined at 25 °C, 45°C, 50 °C, 55 °C, and 60 °C, with linear regression (d) four naphthalenes (top) and four azulenes (bottom) were arranged as observed in the central part of the X-ray structure of [2**BEN14**@Pd_4**AZU1**$_8$] (with respect to the nearest CH-π contacts) and association energies as well as electrostatic potential maps computed (max/min values given for π-surfaces and terminal hydrogens).

To further investigate the transformation kinetics, we performed variable temperature NMR studies at 25°C, 45°C, 50 °C, 55 °C and 60 °C (Fig. S33-37). 1,3,5-trimethoxybenzene was used as an internal standard. At the higher temperatures, the reaction took between 40 min (at 60 °C) and 100 min (at 45 °C) to complete (Fig. 4a). No intermediate could be observed in the spectra. The cage and tetrahedron signals are clearly separated, indicating a slow exchange in the NMR time scale. The reaction follows a first-order law (Fig. 4b and S39). The rate constants were subjected to an Eyring plot analysis (Fig. 4c), giving an activation enthalpy $\mathbf{\Delta H^{\ddagger}}$ of 77.2 kJ/mol and entropy $\mathbf{\Delta S^{\ddagger}}$ of -64 J/mol·K, thus equating to an activation Gibbs free energy $\mathbf{\Delta G^{\ddagger}}$ of 96.1 kJ/mol at 298K. The negative activation entropy suggests a mechanism where the association of two individual cages to one larger assembly (under loss of degrees of freedom) is rate determining.

Next, computations were performed to evaluate the impact of the square-like arrangement of the four azulenes at the center of the tetrahedron on the stability of the final structure. DFT computations at the ωB97X-D/def2-SVP level showed that four azulene units experience a higher stabilization (−75kJ/mol) when arranged in a square than four naphthalenes in a similar CH-π configuration (−58kJ/mol) (Fig. 4d). We attribute this increase in stabilization to more favorable CH-π interactions between the negatively polarized five-membered rings and the positively polarized seven-membered rings of the azulenes.

All newly synthesized species show some weak fluorescence (Section 2 of Supplementary Information). Moreover, like their parent molecule azulene, they exhibit spectral features that indicate retaining an anti-Kasha fluorescence from their S_2-S_0 transition,[48] overlapping with their S_0-S_1 absorption bands.

Finally, we wondered about the stability of the new tetrahedral species if the guests were to be removed. Would an empty [Pd_4**AZU1**$_8$] still exist, or would the system revert back to the [Pd_2**AZU1**$_4$] cage? In previous examples by Fujita[49] and Klajn,[50] neutral guests were removed from a coordination capsule by washing the cage-guest complex with another solvent. In our case, that technique was not applicable, as both cage and guest are soluble in the same range of solvents. In another example, we previously extracted tightly bound Br^- from quadruply interlocked double cages with Ag^+ salts, precipitating AgBr,[51] but also this strategy was not feasible in the present case.

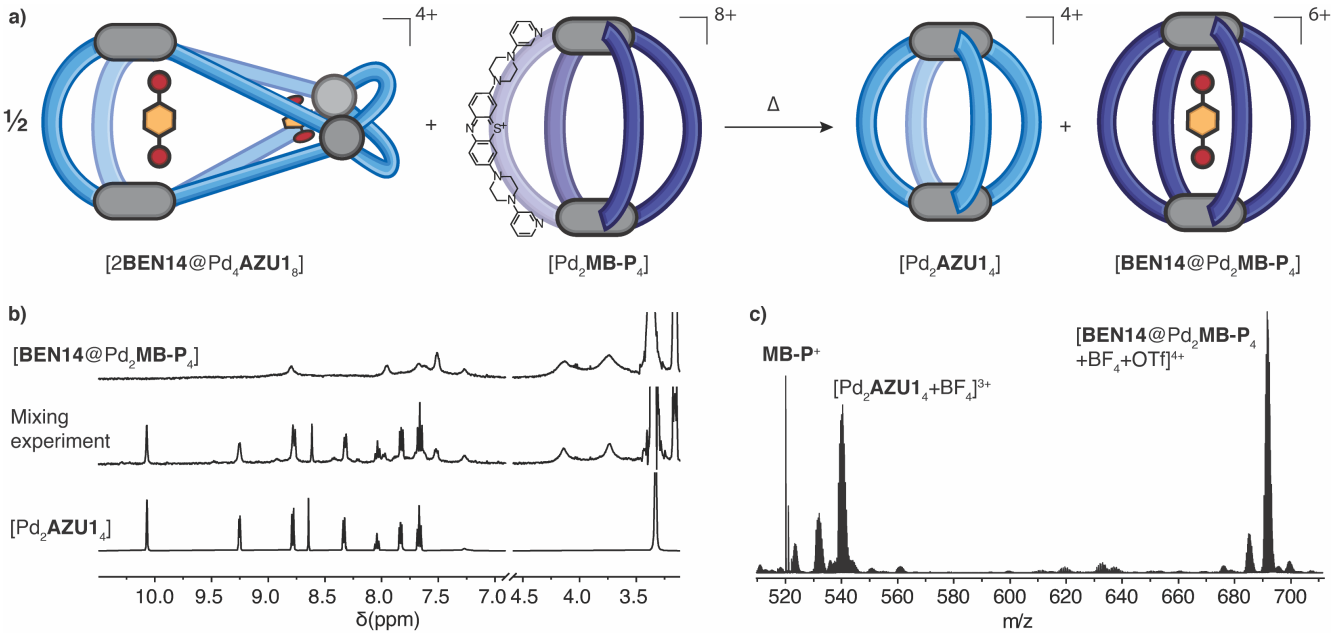

Figure 5: (a) Schematic representation of the guest transfer from tetrahedron [2**BEN14**@Pd$_4$(**AZU1**)$_8$] to the cage [Pd$_2$(**MB-P**)$_4$], yielding cage [Pd$_2$(**AZU1**)$_4$] and host-guest complex [**BEN14**@Pd$_2$(**MB-P**)$_4$]. (b) ^{1}H-NMR spectra (500MHz, 298K, DMSO-d_6) of host-guest complex [**BEN14**@Pd$_2$(**MB-P**)$_4$] (top), cage [Pd$_2$(**AZU1**)$_4$] (bottom), and the result of the transfer experiment, yielding a mixture of the initial cage [Pd$_2$(**AZU1**)$_4$] and host-guest complex [**BEN14**@Pd$_2$(**MB-P**)$_4$] (middle). (c) ESI-MS spectrum of the mixture.

To overcome these limitations, we chose to add another Pd(II)-based cage with increased affinity for the guest as compared to the tetrahedron. In view of the dynamic nature of Pd(II) coordination bonds, we had to select a species that would narcissistically self-sort in the presence of [Pd$_2$**AZU1**$_4$]. A screen of already known cages yielded that previously synthesized methylene blue-based cage [Pd$_2$**MB-P**$_4$][52] does not exchange components with [Pd$_2$**AZU1**$_4$], evidenced by the absence of any scrambling when a mixture of the cages in 1:1 ratio was heated at 70 °C for 15 minutes. As each **MB-P** ligand carries a positive charge, we assumed that the 8+ charge of cage [Pd$_2$**MB-P**$_4$] could favor the uptake of the anionic guests, thus releasing them from [2**BEN14**@Pd$_4$**AZU1**$_8$] (Fig. 5a). A UV/Vis titration of the methylene blue-based cage with **BEN14** indeed indicated strong interaction, but difficulties in fitting the data to a 1:1 or 1:2 binding model precluded us to obtain a reliable binding constant (Fig. S47). Nevertheless, the guest transfer experiment between the cages was successful: when a mixture of [2**BEN14**@Pd$_4$**AZU1**$_8$] and [Pd$_2$**MB-P**$_4$] in 1:2 ratio was heated for 60 minutes at 70 °C, ^{1}H-NMR analysis showed a complete re-transformation of the tetrahedron into the cage (Fig. 5b and S45), as evident by the disappearance of the 1:1 splitting pattern of the tetrahedron and rise of the signals of [Pd$_2$**AZU1**$_4$]. An ESI-MS experiment confirmed the formation of [**BEN14**@Pd$_2$**MB-P**$_4$] and the initial [Pd$_2$**AZU1**$_4$] cage (Fig. 5c and S48). Hence, the data unambiguously demonstrated that the system is reversible and that the geometry of the assembly based on the **AZU1** ligands is controlled by the presence or absence of the disulfonate guest molecules.

CONCLUSION

In conclusion, we prepared three new [Pd$_2$**L**$_4$] assemblies with backbones based on aromatic hydrocarbon azulene and different donor sites, controlling their cavity volume and guest binding behavior. The smallest assembly, lantern-shaped cage [Pd$_2$**AZU1**$_4$] undergoes an unprecedented, rapid and full transformation into tetrahedron [2**G**@Pd$_4$**AZU1**$_8$] upon stoichiometric addition of guest molecules **BEN14** or **BEN13**. The transformation can be reversed by guest re-capture via addition of an octacationic [Pd$_2$**L**$_4$] cage, based on the dye methylene blue. The peculiar electronic structure of the azulene chromophores in the ligand backbones has two implications on the assembly of the studied complexes: pronounced color dependence towards their molecular environment allows to easily follow the transformations by the naked eye as well as UV/Vis spectroscopy. In addition, DFT calculations suggest that favorable CH-π interactions between the four central azulene units stabilize the tetrahedral structure.

The herein established quantitative guest-induced transformation and the possibility to fully reverse this process by adding a higher-charged, non-shuffling [Pd$_2$**L**$_4$] cage enable to embed these assemblies into 'complex systems' with stimuli-responsive behavior. Furthermore, they bear potential for application in cyclic compound separation processes, receptors with visual readout and – owing to azulene's anti-Kasha fluorescence properties– in optoelectronic materials.[53]

ASSOCIATED CONTENT

Synthetic procedures, NMR, MS, UV-Vis spectroscopic data, SCXRD results and DFT calculation data are included in the Supporting Information. CCDC numbers: 2256445, 2256446, 2256447, 2256448 contain the crystallographic data. This material is available free of charge via the Internet at http://pubs.acs.org.

AUTHOR INFORMATION

Corresponding author

* Guido H. Clever – email: guido.clever@tu-dortmund.de

Author Contributions

All authors have given approval to the final version of the manuscript.

Funding Sources

This work was supported by the Deutsche Forschungsgemeinschaft (DFG) trough GRK2376 ("Confinement-Controlled Chemistry", project number 331085229).

AKNOWLEDGMENTS

Dedicated to Prof. Dr. Dietmar Stalke on the occasion of his 65th birthday.
Diffraction data of [Pd_2**AZU1**$_4$], [Pd_2**AZU2**$_4$], [**BEN14**@Pd_2**AZU3**$_4$] and [2**BEN14**@Pd_4**AZU1**$_8$] was collected at PETRA III, DESY (Hamburg, Germany), a member of the Helmholtz Association (HGF). We thank Helena Taberman and Guillaume Pompidor for assistance at synchrotron beamline P11 (I-20200916, STP-20010307, I-20210921 and I-20211437).[54] We thank Prof. Dr. Wolf G. Hiller and his team for help with the NMR measurements, and Dr. Anaya Baksi and Laura Schneider for their help with the ESI-MS measurements.

REFERENCES

(1) Pullen, S.; Tessarolo, J.; Clever, G. H. Increasing Structural and Functional Complexity in Self-Assembled Coordination Cages. Chem. Sci. **2021**, 12, 7269–7293.

(2) McMorran, D. A.; Steel, P. J. The First Coordinatively Saturated, Quadruply Stranded Helicate and Its Encapsulation of a Hexafluorophosphate Anion. *Angew. Chem. Int. Ed.* **1998**, *37*, 3295–3297.

(3) Chand, D. K.; Biradha, K.; Fujita, M. Self-Assembly of a Novel Macrotricyclic Pd(II) Metallocage Encapsulating a Nitrate Ion. *Chem. Commun.* **2001**, 1652–1653.

(4) Clever, G. H.; Tashiro, S.; Shionoya, M. Inclusion of Anionic Guests inside a Molecular Cage with Palladium(II) Centers as Electrostatic Anchors. *Angew. Chem. Int. Ed.* **2009**, *48*, 7010–7012.

(5) Han, M.; Engelhard, D. M.; Clever, G. H. Self-Assembled Coordination Cages Based on Banana-Shaped Ligands. *Chem. Soc. Rev.* **2014**, *43*, 1848–1860.

(6) Harris, K.; Fujita, D.; Fujita, M. Giant Hollow M_nL_{2n} Spherical Complexes: Structure, Functionalisation and Applications. *Chem. Commun.* **2013**, *49*, 6703–6712.

(7) Stang, P. J.; Cao, D. H. Transition Metal Based Cationic Molecular Boxes. Self-Assembly of Macrocyclic Platinum(II) and Palladium(II) Tetranuclear Complexes. *J. Am. Chem. Soc.* **1994**, *116*, 4981–4982.

(8) Fujita, M.; Sasaki, O.; Mitsuhashi, T.; Fujita, T.; Yazaki, J.; Yamaguchi, K.; Ogura, K. On the Structure of Transition-Metal-Linked Molecular Squares. *Chem. Commun.* **1996**, 1535–1536.

(9) Mal, P.; Schultz, D.; Beyeh, K.; Rissanen, K.; Nitschke, J. R. An Unlockable–Relockable Iron Cage by Subcomponent Self-Assembly. *Angew. Chem. Int. Ed.* **2008**, *47*, 8297–8301.

(10) Tessarolo, J.; Lee, H.; Sakuda, E.; Umakoshi, K.; Clever, G. H. Integrative Assembly of Heteroleptic Tetrahedra Controlled by Backbone Steric Bulk. *J. Am. Chem. Soc.* **2021**, *143*, 6339–6344.

(11) Saalfrank, R. W.; Stark, A.; Peters, K.; Schnering, H. G. von. The First "Adamantoid" Alkaline Earth Metal Chelate Complex: Synthesis, Structure, and Reactivity. *Angew. Chem. Int. Ed.* **1988**, *27*, 851–853.

(12) Engelhard, D. M.; Freye, S.; Grohe, K.; John, M.; Clever, G. H. NMR-Based Structure Determination of an Intertwined Coordination Cage Resembling a Double Trefoil Knot. *Angew. Chem. Int. Ed.* **2012**, *51*, 4747–4750.

(13) Fielden, S. D. P.; Leigh, D. A.; Woltering, S. L. Molecular Knots. *Angew. Chem. Int. Ed.* **2017**, *56*, 11166–11194.

(14) Forgan, R. S. R.; Sauvage, J.-P. J.; Stoddart, J. F. J. Chemical Topology: Complex Molecular Knots, Links, and Entanglements. *Chem. Rev.* **2011**, *111*, 5434–5464.

(15) Ashbridge, Z.; Kreidt, E.; Pirvu, L.; Schaufelberger, F.; Stenlid, J. H.; Abild-Pedersen, F.; Leigh, D. A. Vernier Template Synthesis of Molecular Knots. *Science* **2022**, *375*, 1035–1041.

(16) Bloch, W. M.; Holstein, J. J.; Dittrich, B.; Hiller, W.; Clever, G. H. Hierarchical Assembly of an Interlocked M_8L_{16} Container. *Angew. Chem. Int. Ed.* **2018**, *57*, 5534–5538.

(17) Au-Yeung, H. Y.; Deng, Y. Distinctive Features and Challenges in Catenane Chemistry. *Chem. Sci.* **2022**, *13*, 3315–3334.

(18) Evans, N. H.; Beer, P. D. Progress in the Synthesis and Exploitation of Catenanes since the Millennium. *Chem. Soc. Rev.* **2014**, *43*, 4658–4683.

(19) Percástegui, E. G.; Mosquera, J.; Nitschke, J. R. Anion Exchange Renders Hydrophobic Capsules and Cargoes Water-Soluble. *Angew. Chem. Int. Ed.* **2017**, *56*, 9136–9140.

(20) Kim, T. Y.; Vasdev, R. A. S.; Preston, D.; Crowley, J. D. Strategies for Reversible Guest Uptake and Release from Metallosupramolecular Architectures. *Chem. Eur. J.* **2018**, *24*, 14878–14890.

(21) Ward, M. D.; Hunter, C. A.; Williams, N. H. Coordination Cages Based on Bis(Pyrazolylpyridine) Ligands: Structures, Dynamic Behavior, Guest Binding, and Catalysis. *Acc. Chem. Res.* **2018**, *51*, 2073–2082.

(22) Ronson, T. K.; Carpenter, J. P.; Nitschke, J. R. Dynamic Optimization of Guest Binding in a Library of Diastereomeric Heteroleptic Coordination Cages. *Chem* **2022**, *8*, 557–568.

(23) Xue, Y.; Hang, X.; Ding, J.; Li, B.; Zhu, R.; Pang, H.; Xu, Q. Catalysis within Coordination Cages. *Coord. Chem. Rev.* **2020**, *430*, 213656.

(24) Scherer, M.; Caulder, D. L.; Johnson, D. W.; Raymond, K. N. Triple Helicate—Tetrahedral Cluster Interconversion Controlled by Host–Guest Interactions. *Angew. Chem. Int. Ed.* **1999**, *38*, 1587–1592.

(25) Wood, D. M.; Meng, W.; Ronson, T. K.; Stefankiewicz, A. R.; Sanders, J. K. M.; Nitschke, J. R. Guest-Induced Transformation of a Porphyrin-Edged $Fe^{II}_4L_6$ Capsule into a $Cu^{I}Fe^{II}_2L_4$ Fullerene Receptor. *Angew. Chem. Int. Ed.* **2015**, *54*, 3988–3992.

(26) Zhu, R.; Lübben, J.; Dittrich, B.; Clever, G. H. Stepwise Halide-Triggered Double and Triple Catenation of Self-Assembled Coordination Cages. *Angew. Chem. Int. Ed.* **2015**, *54*, 2796–2800.

(27) Zhang, T.; Zhou, L.-P.; Guo, X.-Q.; Cai, L.-X.; Sun, Q.-F. Adaptive Self-Assembly and Induced-Fit Transformations of Anion-Binding Metal-Organic Macrocycles. *Nat. Commun.* **2017**, *8* , ncomms15898.

(28) Sekiya, R.; Fukuda, M.; Kuroda, R. Anion-Directed Formation and Degradation of an Interlocked Metallohelicate. *J. Am. Chem. Soc.* **2012**, *134*, 10987–10997.

(29) Percástegui, E. G. Guest-Induced Transformations in Metal-Organic Cages. *Eur. J. Inorg. Chem.* **2021**, *2021*, 4425–4438.

(30) Benchimol, E.; Nguyen, B.-N. T.; Ronson, T. K.; Nitschke, J. R. Transformation Networks of Metal–Organic Cages Controlled by Chemical Stimuli. *Chem. Soc. Rev.* **2022**, *51*, 5101–5135.

(31) Liu, H.-K.; Ronson, T. K.; Wu, K.; Luo, D.; Nitschke, J. R. Anionic Templates Drive Conversion between a $Zn^{II}_9L_6$ Tricapped Trigonal Prism and $Zn^{II}_6L_4$ Pseudo-Octahedra. *J. Am. Chem. Soc.* **2023**, *145*, 15990–15996.

(32) Sekiya, R.; Fukuda, M.; Kuroda, R. Anion-Directed Formation and Degradation of an Interlocked Metallohelicate. *J. Am. Chem. Soc.* **2012**, *134*, 10987–10997.

(33) Anderson, A. G.; Steckler, B. M. Azulene. VIII. A Study of the Visible Absorption Spectra and Dipole Moments of Some 1- and 1,3-Substituted Azulenes. *J. Am. Chem. Soc.* **1959**, *81*, 4941–4946.

(34) Michl, J.; Thulstrup, E. W. Why Is Azulene Blue and Anthracene White? A Simple MO Picture. *Tetrahedron* **1976**, *32* 205–209.

(35) Anderson, A. G.; Nelson, J. A.; Tazuma, J. J. Azulene. III. Electrophilic Substitution 1-3. *J. Am. Chem. Soc.* **1953**, *75*, 4980–4989.

(36) Lee, H.; Tessarolo, J.; Langbehn, D.; Baksi, A.; Herges, R.; Clever, G. H. Light-Powered Dissipative Assembly of Diazocine Coordination Cages. *J. Am. Chem. Soc.* **2022**, *7*, 3099–3105.

(37) Chen, B.; Holstein, J. J.; Platzek, A.; Schneider, L.; Wu, K.; Clever, G. H. Cooperativity of Steric Bulk and H-Bonding in Coordination Sphere Engineering: Heteroleptic Pd^{II} Cages and Bowls by Design. *Chem. Sci.* **2022**, *13*, 1829–1834.

(38) Hasegawa, S.; Meichsner, S. L.; Holstein, J. J.; Baksi, A.; Kasanmascheff, M.; Clever, G. H. Long-Lived C60 Radical Anion Stabilized Inside an Electron-Deficient Coordination Cage. *J. Am. Chem. Soc.* **2021**, *143*, 9718–9723.

(39) Bloch, W. M.; Horiuchi, S.; Holstein, J. J.; Drechsler, C.; Wuttke, A.; Hiller, W.; Mata, R. A.; Clever, G. H. Maximized Axial Helicity in a Pd_2L_4 Cage: Inverse Guest Size-Dependent Compression and Mesocate Isomerism. *Chem. Sci.* **2023**, *14*, 1524–1531.

(40) Liu, R. S. H. Colorful Azulene and Its Equally Colorful Derivatives. *J. Chem. Educ.* **2002**, *79*, 183.

(41) Zieliński, T.; Kędziorek, M.; Jurczak, J. The Azulene Moiety as a Chromogenic Building Block for Anion Receptors. *Tetrahedron Lett.* **2005**, *46*, 6231–6234.

(42) Clever, G. H.; Punt, P. Cation–Anion Arrangement Patterns in Self-Assembled Pd2L4 and Pd4L8 Coordination Cages. *Acc. Chem. Res.* **2017**, *50*, 2233–2243.

(43) Bloch, W. M.; Abe, Y.; Holstein, J. J.; Wandtke, C. M.; Dittrich, B.; Clever, G. H. Geometric Complementarity in Assembly and Guest Recognition of a Bent Heterolepticcis-$[Pd_2LA_2LB_2]$ Coordination Cage. *J. Am. Chem. Soc.* **2016**, *138*, 13750–13755.

(44) Jansze, S. M.; Cecot, G.; Wise, M. D.; Zhurov, K. O.; Ronson, T. K.; Castilla, A. M.; Finelli, A.; Pattison, P.; Solari, E.; Scopelliti, R.; Zelinskii, G. E.; Vologzhanina, A. V.; Voloshin, Y. Z.; Nitschke, J. R.; Severin, K. Ligand Aspect Ratio as a Decisive Factor for the Self-Assembly of Coordination Cages. *J. Am. Chem. Soc.* **2016**, *138*, 2046–2054.

(45) Sudan, S.; Fadaei-Tirani, F.; Scopelliti, R.; Ebbert, K. E.; Clever, G. H.; Severin, K. LiBF4-Induced Rearrangement and Desymmetrization of a Palladium-Ligand Assembly. *Angew. Chem. Int. Ed.* **2022**, *61*, e202201823.

(46) Klein, C.; Gütz, C.; Bogner, M.; Topić, F.; Rissanen, K.; Lützen, A. A New Structural Motif for an Enantiomerically Pure Metallosupramolecular Pd4L8 Aggregate by Anion Templating. *Angew. Chem. Int. Ed.* **2014**, *53*, 3739–3742.

(47) Ibáñez, S.; Peris, E. Dimensional Matching versus Induced-Fit Distortions: Binding Affinities of Planar and Curved Polyaromatic Hydrocarbons with a Tetragold Metallorectangle. *Angew. Chem. Int. Ed.* **2020**, *59*, 6860–6865.

(48) Beer, M.; Longuet-Higgins, H. C. Anomalous Light Emission of Azulene. J. Chem. Phys. **1955**, *23*, 1390–1391.

(49) Wang, S.; Sawada, T.; Ohara, K.; Yamaguchi, K.; Fujita, M. Capsule–Capsule Conversion by Guest Encapsulation. *Angew. Chem. Int. Ed.* **2016**, *55*, 2063–2066.

(50) Hema, K; Grommet, A. B.; Białek, M. J.; Wang, J.; Schneider, L.; Drechsler, C.; Yanshyna, O.; Diskin-Posner, Y.; Clever, G. H.; Klajn, R. Guest Encapsulation Alters the Thermodynamic Landscape of a Coordination Host. *J. Am. Chem. Soc.* **2023**, DOI: 10.1021/jacs.3c08666.

(51) Freye, S.; Hey, J.; Torras-Galán, A.; Stalke, D.; Herbst-Irmer, R.; John, M.; Clever, G. H. Allosteric Binding of Halide Anions by a New Dimeric Interpenetrated Coordination Cage. *Angew. Chem. Int. Ed.* **2012**, *51*, 2191–2194.

(52) Regeni, I.; Chen, B.; Frank, M.; Baksi, A.; Holstein, J. J.; Clever, G. H. Coal-Tar Dye-Based Coordination Cages and Helicates. *Angew. Chem. Int. Ed.* **2021**, *60*, 5673–5678.

(53) Xin, H.; Gao, X. Application of Azulene in Constructing Organic Optoelectronic Materials: New Tricks for an Old Dog. *ChemPlusChem* **2017**, *82*, 945–956.

(54) Burkhardt, A.; Pakendorf, T.; Reime, B.; Meyer, J.; Fischer, P.; Stübe, N.; Panneerselvam, S.; Lorbeer, O.; Stachnik, K.; Warmer, M.; Rödig, P.; Göries, D.; Meents, A. Status of the Crystallography Beamlines at PETRA III. *Eur. Phys. J. Plus* **2016**, *131*, 56.